$InSb/LiNbO_3$ acoustoelectric convolver operating at 77 K," *Appl. Phys. Lett.*, vol. 33, pp. 484–486, Sept. 1978.
[22] J. H. Cafarella, private communication.
[23] T. M. Reeder, W. S. Shreve, and P. L. Adams, "A new broadband coupling network for interdigital surface wave transducers," *IEEE Trans. Sonics Ultrason.*, vol. SU-19, pp. 466–477, Oct. 1972.
[24] I. Yao, private communication.
[25] J. H. Holtham and R. C. Williamson, "Automatic pulsed technique for measuring phase and amplitude response of SAW devices," in *1978 IEEE Proc. Ultrasonics Symp.*, pp. 607–610.
[26] E. L. Adler, "Electromagnetic Long-Line Effects In SAW Convolvers," in *1980 IEEE Proc. Ultrasonics Symp.*, to be published.
[27] See, for example, M. Schwartz, W. R. Bennett, and S. Stein, *Communication Systems and Techniques*. New York: McGraw-Hill, 1966, p. 67.
[28] J. H. Cafarella, "Device requirements for spread-spectrum communication," in *Optical Signal Processing for C^3I*, Bellingham, WA: SPIE, 1979, vol. 209, pp. 53–56.

An Application of SAW Convolvers to High Bandwidth Spread Spectrum Communications

JEFFREY H. GOLL, MEMBER, IEEE, AND DONALD C. MALOCHA, MEMBER, IEEE

Abstract—**A spread spectrum communications subsystem that is based on the separated medium acoustoelectric convolver is described. The subsystem generates minimum-shift-keyed (MSK) waveforms with the aid of SAW filters and performs differential-phase-shift-keyed (DPSK) data demodulation with acoustoelectric convolvers. The convolver provides a *BT* product of 2200 with a 3-dB bandwidth of 100 MHz. The signals processed by the subsystem have a *BT* product of 1100. In this paper, the subsystem, the generation of MSK waveforms, and the use of acoustoelectric convolvers are described. Important subsystem performance characteristics, including dynamic range ($\simeq$50 dB), contribution to implementation loss ($\simeq$1 dB), DPSK demodulation, and distortion levels are illustrated and discussed.**

I. Introduction

THE ACOUSTOELECTRIC convolver [1], [2] is a programmable matched filter with a unique combination of demonstrated large processing gain, good dynamic range, broad bandwidth, small size and weight, and low drive power requirements. It provides the central component for a high data rate spread spectrum communications receiver. A convolver-based system can provide secure spread spectrum communications [3] with fast synchronization [4], low probability of intercept transmission, and good jammer immunity. In contrast with conventional matched filters based on surface acoustic wave (SAW) tapped delay lines, the convolver processing gain is virtually independent of temperature. Decoding of differential-phase-shift-keyed (DPSK) data can be conveniently accomplished with a dual convolver [5]. Wide-band minimum-phase-shift-keyed (MSK) waveforms for use with the convolver can be generated with the aid of an appropriately designed SAW filter [6].

Highly developed gap-coupled acoustoelectric convolvers [5], [7]–[9] provide processing gains of up to 33 dB with adequate dynamic range and input bandwidths of 100 MHz. Recently, an acoustoelectric convolver with an input bandwidth of 200 MHz has been demonstrated [10]. The mechanical support structure of the device insures stable operation over a 100°C temperature range [5], [10]. Such devices have passed stringent vibration tests for military

Manuscript received April 24, 1980; revised September 22, 1980. This work was supported by the Defense Advanced Research Projects Agency and the Department of the Army.

J. H. Goll is with the Central Research Laboratories, Texas Instruments Inc., Dallas, TX 75265.

D. C. Malocha was with the Central Research Laboratories, Texas Instruments Inc., Dallas, TX. He is now with Sawtek Inc., Orlando, FL 32854.

0018-9480/81/0500-0473$00.75 ©1981 IEEE

aircraft, jeeps, and tracked-vehicle equipment [10], [11].

A convolver-based spread spectrum subsystem has been developed at Lincoln laboratory and Texas Instruments for the DARPA Upgraded Packet Radio Program [12]. Initial development of devices and prototype systems took place at Lincoln Laboratory. Texas Instruments has continued the development of devices and systems and has constructed eight subsystems for the Upgraded Packet Radio. These subsystems differ from the Lincoln Laboratory prototypes in three ways. First, they utilize the improvements [6]–[9] in device and system design that were developed since the construction of the prototypes. Second, the subsystem has been reduced to a printed-circuit board implementation that is easily produced. Finally, subsystem power consumption has been reduced by taking advantage of improved convolver efficiency and selecting more efficient components.

In the remainder of this paper the construction, use in data communication, and performance of the subsystem are described. In Section II acoustoelectric convolvers, the methods of data communication employed in the convolver-based subsystem, and the design of the transmitter and receiver using this subsystem are described. The generation of MSK waveforms using a SAW MSK filter and the use of this filter to compensate for distortions created by the high-speed electronics of the waveform generator are described in Section III and the Appendix. Finally, the performance of the subsystem is illustrated in Section IV.

II. Convolver-Based Spread Spectrum Communications System

In the system described here, data demodulation is accomplished using DPSK [13]. Many specific features of the system implementation are determined by the characteristics of the convolver and the choice of DPSK.

The convolver devices used in this application are illustrated in Fig. 1. Each device consists of a SAW delay line fabricated on $LiNbO_3$, separated by a small air gap ($\simeq 0.5$ μm) from two bars of silicon, each approximately 3.8 cm, or 11 μs long. Two input signals, the signal $S(t)$ and the reference $R(t)$, are applied to the input interdigital SAW transducers at the two ends of the $LiNbO_3$. As the two signals counterpropagate beneath the silicon, the electric fields that accompany them interact nonlinearly with charge carriers near the silicon surface. The resulting output

$$C(t)=k\int S(\tau)R(2t-\tau-T)\,d\tau \qquad (1)$$

where T is the total delay time beneath the silicon, is a time-compressed replica of the convolution of the two input signals. If one of the inputs is time reversed, the output is the correlation rather than the convolution of the two inputs, and therefore the device provides the matched filter function [13]. It is freely programmable, constrained only by its length and the bandwidth of the input SAW transducers.

Each bar of silicon is 1 bit period in length. The outputs from the two bars are the matched filter functions for two successive bit periods. Therefore, the device geometry provides a natural means for DPSK demodulation: the 1-bit delay time required to compare successive bits is built into the device.

The essential elements of the convolver-based spread spectrum system are illustrated in Figs. 1 and 2. The Upgraded Packet Radio subsystem consists of an MSK modulator board for waveform generation and a convolver board for matched filtering and DPSK demodulation. The contents of these circuit boards are highlighted in Figs. 1 and 2.

The transmitter (Fig. 2(a)) utilizes MSK [14], [15] waveforms. A high data rate digital code, called the chip code, is generated at a rate $f_c=1/T_c$, where T_c is the chip duration. In the subsystem under discussion, $f_c\simeq 92.5$ MHz and $T_c\simeq 10.8$ ns. The details of the chip code are determined by cryptographic requirements. This code is superimposed on a carrier by the MSK modulator (see Section III). Each bit period, of length T_b ($\simeq 11$ μs), contains N ($=1024$) chips. A bit code $b_n'(t)$, containing the binary encoded message to be transmitted, is also superimposed on the MSK waveform. The bit rate is $f_b\simeq 91$ kHz. The phase of the MSK modulator output is controlled by a code $b_n(t)$, derived from the bit code. Over intervals of length T_b, the phase of the MSK waveform is shifted by π radians or not shifted, depending on $b_n(t)$. (Details of this procedure may be found in [13].) In this way, the digital information to be communicated, $b_n'(t)$, is built into the relative phase of consecutive bits of the transmitted waveform.

In the receiver (Fig. 2(b)), SAW convolvers are used to decipher the chip code and to achieve processing gain. A chip code generator and an MSK modulator supply a reference MSK input to the convolver. The other convolver input is derived from the received signal. The reference MSK waveform differs from the signal in several respects. First, no bit-level code is used in the reference. This is central to bit demodulation: since there are "phase flips" controlled by the transmitter only, the matched filter output phase is controlled uniquely by the transmitted waveform. Detection of this phase allows determination of the original bit information. Second, within a given bit, the chip code in the reference is the time reverse of the chip code of the corresponding bit in the signal. That is, if each bit has N chips, the nth chip in the signal is the same as the $(1+N-n)$th chip in the reference. This feature is a result of the time-reversal requirement described earlier. Third, the kth bit precedes the $(k+1)$th bit in the signal, but follows it in the reference. This is a result of the implementation of DPSK demodulation using two convolvers on one substrate, as described earlier. With this device architecture, the kth bit of both the signal and the reference must line up beneath the rightmost silicon bar in Fig. 1 at the same time as the $(k+1)$th bits of the signal and reference line up beneath the leftmost silicon bar. A further consequence of this alignment requirement is that a single device

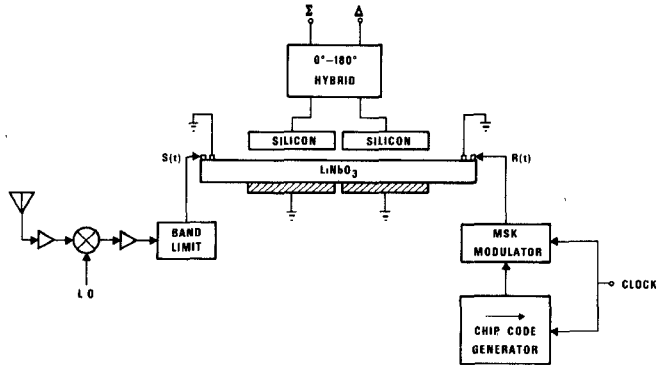

Fig. 1. Schematic diagram of a convolver as part of a DPSK spread spectrum receiver. The arrows drawn in the chip code generators in Figs. 1 and 2 indicate the direction in time of the code (see text).

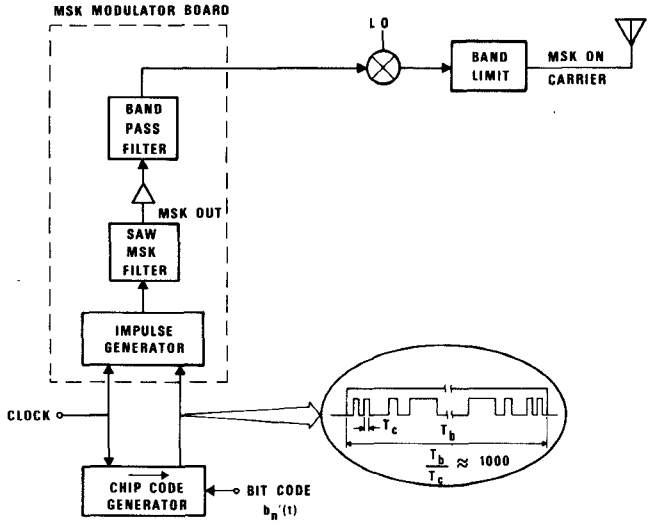

(a)

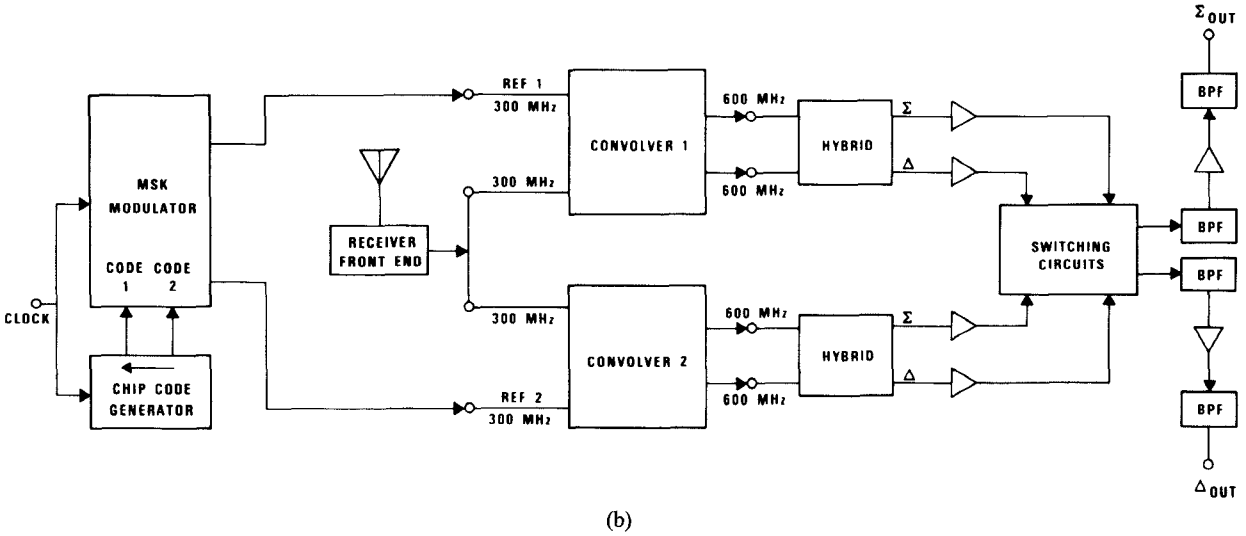

(b)

Fig. 2. (a) Block diagram of a convolver-based DPSK spread spectrum system transmitter, highlighting the contents of the MSK modulator board. (b) Receiver, with two channels for 100-percent duty cycle operation. The convolver board contains two convolvers and all components of this diagram to the right of the convolvers.

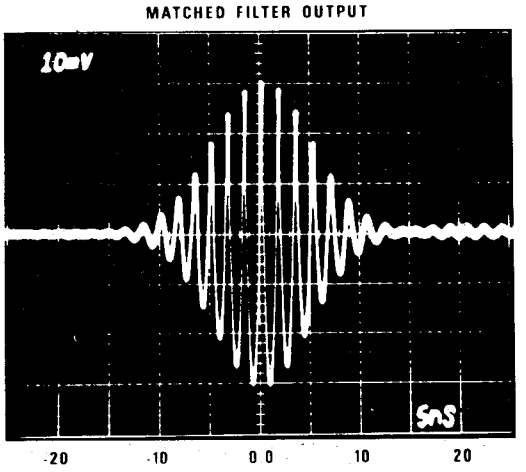

Fig. 3. Matched filter output, representing the convolution of two 22-μs-long MSK signals. Note that the ideal response would be $\simeq$22 ns wide to the nulls of the main response.

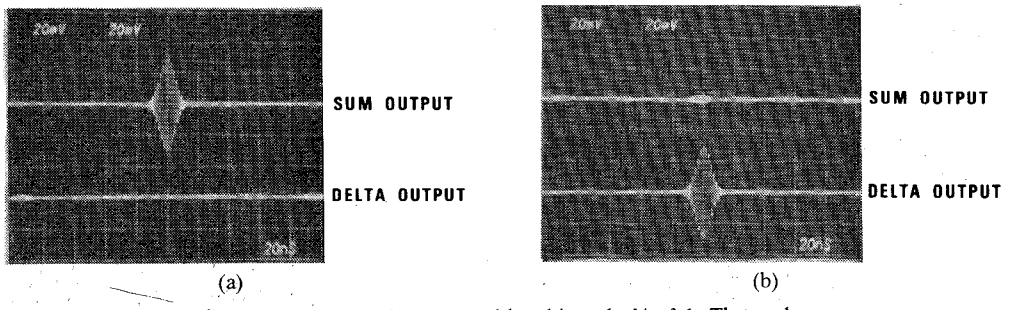

(a) (b)

Fig. 4. (a) DPSK performance with a bit code b'_n of 1. The peak sum output (top trace) is more than 20 dB larger than the delta output (bottom trace). (b) DPSK performance with a bit code b'_n of 0. The delta output is more than 20 dB larger than the sum output.

can process only 50 percent of the transmitted data. Therefore, in order to achieve 100-percent duty cycle operation of the receiver, two identical channels are used and selection switches are included (Fig. 2(b)). Convolver 1 performs DPSK demodulation using bits 1 and 2, 3 and 4, etc. (using a reference waveform with a bit sequence 2, 1, 4, 3, etc.). Convolver 2 processes bits 2 and 3, 4 and 5, etc. (using a reference code in order 3, 2, 5, 4, etc.). Two separate MSK generation channels are used to supply the two convolvers with the required reference waveforms.

Given the convolver geometry of Fig. 1, DPSK demodulation is easily done. The matched filter output of a typical bit period is illustrated in Fig. 3. This RF waveform has a well-defined phase. Outputs corresponding to successive bit periods are generated simultaneously in the two halves of a convolver. These two outputs are either identical or they differ by a phase shift of π radians, depending on the transmitter bit code. Thus data demodulation can be achieved by simply adding and subtracting the two convolver outputs from one DPSK convolver in a 180° hybrid. Depending on the bit-level phase shifts introduced in the transmitter, either the Σ output is large and the Δ small (nominally zero), giving data 1, or vice versa, giving data 0. The performance of a typical subsystem under these two conditions is illustrated in Fig. 4. A large ratio of the sum and delta outputs (sum/delta for data 1 and delta/sum for data 0) is desired to minimize the impact on system bit error rates. The typical measured value of 20 dB exceeds the system specification of 14 dB.

The convolver output is developed at twice the input frequency. Consequently, spurious output due to electromagnetic feedthrough can be suppressed by bandpass filters. Inputs and outputs of the convolvers are centered at 300 and 600 MHz, respectively. Feedthrough of input signals directly to the output is suppressed by the two bandpass filters—a four pole and a one pole—in the convolver board (Fig. 2(b)). These filters in cascade are designed for 180-MHz 3-dB bandwidth, centered at 600 MHz and more than 55-dB rejection across the input frequency band. Assuming 60-dB suppression of feedthrough in the convolver and +15-dBm maximum input signals, this 55-dB rejection is sufficient to limit the output signal-to-noise degradation due to 300-MHz feedthrough to less than 0.5 dB. These filters also reduce transients

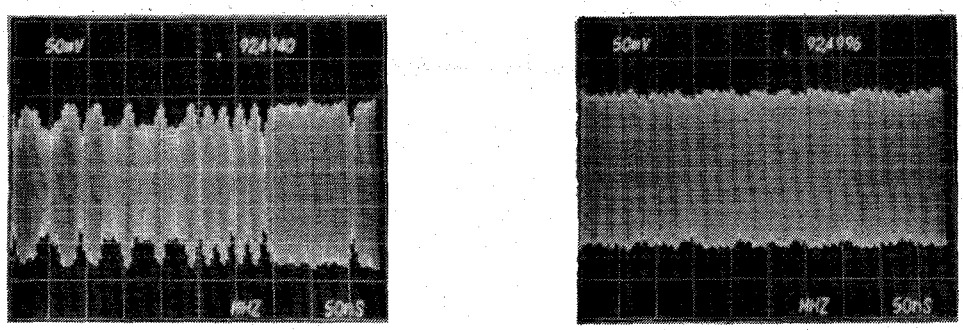

(a) (b)

Fig. 5. Outputs of the MSK modulator board. (a) Distorted MSK, before implementation of the compensated MSK filter. (b) Improved MSK waveforms, generated using the compensated SAW MSK filter.

from the switching circuitry and prevent possible saturation of the output amplifiers. Therefore, the four-pole filter is placed immediately after the switches. The one-pole filter is placed after the final amplifier to reestablish the desired noise bandwidth. Similarly, a five-pole bandpass filter with a 3-dB bandwidth of 120 MHz centered at 300 MHz is included in the modulator board (Fig. 2(a)). This filter limits the second-harmonic content of the MSK reference waveforms to -40 dBm or less. The degradation of signal-to-noise ratio at the convolver board output due to spurious input signals in the 600-MHz band is thereby limited to less than 0.5 dB.

The measured degradation of the system noise floor due to electromagnetic feedthrough, including all frequencies, was typically less than 0.5 dB.

III. Generation of High Bandwidth MSK Waveforms

MSK waveforms are characterized by tighter spectral confinement than the more commonly used phase-shift-keyed (PSK) waveforms. More than 99.5 percent of the MSK energy is located between the first nulls of the MSK spectrum, compared to 92 percent for PSK waveforms. Therefore, MSK is a desirable waveform for multichannel systems. SAW filters offer the broad bandwidth and precise control of impulse response required for MSK waveform generation. Two techniques for generating MSK using SAW filters have been reported. One, [6], [17], based on an impulse generator together with a SAW filter, is utilized in the convolver-based subsystem and is described in detail in the Appendix. The other [18] uses a SAW filter for conversion of PSK to MSK. The impulse generator technique is more fully developed and has been used to produce waveforms with low distortion levels at chipping rates as high as 92.5 MHz. Provided system clocks are available at the required rates, the PSK-to-MSK conversion scheme appears simpler to implement. It is inherently more efficient, since the energy of the PSK waveform input to the SAW filter is concentrated in the passband of the filter, whereas an impulse has much of its energy outside the passband of the corresponding filter. This simplifies the circuit implementation by reducing the required gain. In addition, the PSK-to-MSK conversion scheme should suffer smaller distortions as a result of timing jitter in the data transitions. However, the authors are not aware of any published records of MSK waveforms produced with this technique. The SAW PSK-to-MSK conversion filter in [18] was designed for a chipping rate of only 5 MHz. Therefore, in comparing the two techniques, the high-bandwidth low-distortion results reported here should be considered along with the potential advantages of the PSK-to-MSK conversion technique.

The simplest measure of deviation from ideal MSK is amplitude modulation (AM). The system specifications required <20 percent AM, with <10 percent desired. As described in the Appendix, initial implementations of the subsystem did not meet this specification. The MSK waveforms, illustrated in Fig. 5(a), exhibited $\simeq 25$ percent AM. The problem was solved by tailoring the SAW MSK filter passband to compensate for the frequency rolloff of the impulse generator output spectrum. The resulting MSK waveform is illustrated in Fig. 5(b). AM in this case was reduced to $\simeq 7$ percent, with $\simeq 13$ percent typical in the 8 channels made.

IV. Performance of the Convolver-Based Subsystem

The performance achieved with the convolver-based subsystem, consisting of a modulator board and a convolver board as described in Sections II and III, is summarized in Table I. The parameters most relevant for system implementation are emphasized. The data in Table I are based on the measured performance of four subsystems, containing eight convolver devices and eight output channels, built at Texas Instruments. Note that the BT product of the MSK waveforms used in the subsystem—nominally 31 dB—is slightly less than the convolver BT product of 33 dB.

The dynamic range and implementation loss measurements require considerable care and merit further discussion. Matched filter outputs generated by convolution over the entire device length (2 bits, or 22 μs) are used in each

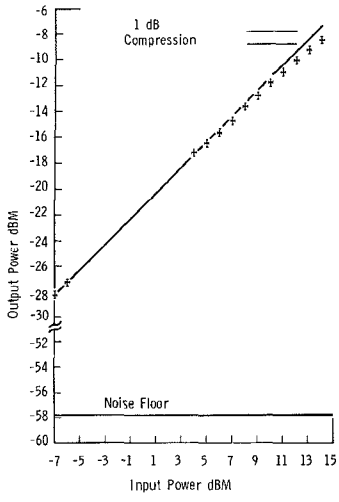

Fig. 6. Plot of CW equivalent output power versus MSK input power for a typical convolver board channel. The dynamic range indicated is approximately 49 dB.

TABLE I
PERFORMANCE OF THE CONVOLVER-BASED DPSK SPREAD SPECTRUM SUBSYSTEM

	Specification	Measurement
A. DPSK Convolver Devices		
Interaction Length (μsec)	22	22 ± .2
Input 3 dB Bandwidth (MHz)	100	100 ± 10
Input Center Frequency (MHz)	300	300
Time-Bandwidth Product	2200	2200
Conversion Efficiency F,[1] (dBm)	>-70	-66 ± 4
Dynamic Range (dB relative to kTB)	--	56 ± 4
Maximum Output Power (P_1=P_2=+15 dBm)	--	-36 ± 4
Input/Output Isolation (dB)	60	63 ± 3
Operating Temperature	-25 to 70°C	-25 to 70°C
Phase deviation from linear	--	±15°
B. Convolver Subsystem: MSK Waveforms		
Maximum Power Out (dBm)	+15	+15 ± 3
3 dB Bandwidth (MHz)	<56	46 ± 3
Waveform Time-Bandwidth Product (dB)	30.9	30.1
AM (%)	<20	13 ± 6
Upper Harmonic Content at Maximum Output (dBm)	--	<-45
DC Power Consumption, MSK Modulator (Watts)[2]	--	4.2 ± .1
Output VSWR	<2:1 across passband	<2:1
C. Convolver Subsystem: Convolver Board		
Dynamic Range (dB)	>40	50 ± 3
Sum/Delta Ratio (dB)	>14	>17
Implementation Loss[3] (dB)	--	1 ± .2
Input Power at 1 dB Compression (dBm, both Signal and Reference)	--	15 ± 2
DC Power Consumption (Watts)	--	1.6 ± .3

[1] Defined as F = 10 log(P_{out}/P_1P_2), where P_{out} is the device output power and P_1 and P_2 are the two input powers, all in mW.

[2] This does not include Chip Code Generator.

[3] Contribution of convolvers and waveform generators only. In addition to the ± .2 dB variations among channels there is a measurement uncertainty estimated at ± .5 dB.

measurement. The signal and reference waveforms are MSK, based on chip codes 22 μs long with appropriate time reversal. The peak instantaneous output signal power, S_{out}, is measured as follows. First the maximum amplitude of the subsystem output (see Fig. 3) is found using an oscilloscope. A CW signal source is used to generate a signal at 600 MHz (the center of the output frequency band) with the same amplitude. The rms power, S_m, of this CW signal is then measured using a power meter. Twice this rms power gives the peak instantaneous output power S_{out}: $S_{out}=2\times S_m$. S_m will be referred to as the CW equivalent output power of the subsystem. The CW equivalent power, C_m, and the peak instantaneous power, C_{out}, at the convolver output can be determined by subtracting the net gain of the post-convolver electronics from S_m and S_{out}, respectively.

The subsystem dynamic range is defined as the difference between the subsystem noise floor and the CW equivalent output power at 1-dB compression. The subsystem noise floor is defined as the rms subsystem output power when a full power reference waveform is applied to each convolver and the signal input ports are terminated. This simulates the case when no signal is received. The 1-dB compression point is determined by measuring the CW equivalent output power S_m as a function of input MSK power S_{in}, with the reference power fixed at its maximum value. A typical result is shown in Fig. 6. The dynamic range of the convolver (generally quoted relative to thermal noise) is similarly determined by measuring, as described above, C_m as a function of S_{in}, locating the 1-dB compression point, and comparing to kTB. Note that the subsystem dynamic range differs from the device dynamic range by about 6 dB. The difference is accounted for by several factors that degrade the signal-to-noise ratio after the device output. These factors include losses in the 180° hybrid (1 ± 0.5 dB), the preamplifier noise figure (3 ± 0.5 dB), and miscellaneous factors (1.5 ± 1 dB) such as residual effects of crosstalk from convolver input to output, the output amplifier noise figure, and failure to achieve exactly the desired noise bandwidth.

The subsystem implementation loss, L_{subsys}, is defined as the difference (in decibels) between the output signal-to-noise ratios of the ideal matched filter and the actual subsystem in the presence of jamming. This loss is a function of many factors, such as signal and noise levels at the input, device efficiency and dynamic range, correlation between the jammer and the signal, and amplifier noise figures. A single, simple figure of merit, L_{conv}, that describes the contribution of the convolvers and waveform generators to the implementation loss can be defined with the aid of two simplifying assumptions. First, since matched filters are ideal when used with white Gaussian noise, band-limited white-noise jammers, with noise equivalent bandwidth B_N and spectral density n_0 will be assumed. Second, to make the figure of merit independent of amplifier noise figures and signal and jammer levels at the input, L_{conv} will be defined in terms of signal and noise levels at the convolver output. Equivalently, only that noise in the signal at the subsystem output is considered that is present because of the jammer at the input. L_{conv} is then defined as

$$L_{conv}=(S/N)_{ideal}/(C_{out}/N_{out}) \quad (2)$$

where $(S/N)_{ideal}$ is the output signal-to-noise ratio of the ideal matched filter, C_{out} is the peak instantaneous output of the convolver, and N_{out} is the rms noise power at the convolver output, excluding thermal noise (kTB).

It is difficult to measure C_{out}/N_{out} when the signal and noise inputs are applied simultaneously. Therefore, the signal and noise inputs are applied separately when measuring C_{out} and N_{out}, respectively. As long as the device is not significantly saturated by one or both inputs, the resulting measurement of L_{conv} is not affected by the separate application of S_{in} and N_{in}. C_{out} is measured as described earlier. N_{out} must be determined indirectly. The power at the subsystem output is first measured when N_{in} is applied at the input. The result includes, in addition to N_{out}, the effects of the post-convolver electronics. These effects, which are dominated by the noise figure of the first amplifier and the gain of all amplifiers, must be subtracted from the measured noise power at the subsystem output to give an estimate of N_{out}.

L_{conv} can be expressed in terms of readily measurable quantities by using the well-known result

$$(S/N)_{ideal}=2E/n_0 \tag{3}$$

where E is the energy in the input signal. E and n_0 are given by

$$E=S_{in}\times T \tag{4}$$

$$n_0=N_{in}/B_N \tag{5}$$

where T is the length of the matched filter and S_{in} and N_{in} are the rms input signal (MSK) and noise powers. Equations (2)–(4) together show that

$$L_{conv}=(2BT)\times(S_{in}/N_{in})/(C_{out}/N_{out}) \tag{6}$$

or, if all power ratios are expressed in decibels

$$L_{conv}=10\log(2BT)+(S_{in}/N_{in})-(C_{out}/N_{out}). \tag{7}$$

The subsystem discrimination against a white-noise jammer can be calculated by adding the effects of the post-convolver electronics to the effects of L_{conv}. Thus by using this single figure of merit to characterize the waveform generators and convolvers, the signal-to-noise ratio expected at the output can be determined for arbitrary input power levels. For jammers other than white, Gaussian noise, the correlations of the code and the jammer must also be taken into account.

A typical measurement of C_{out}/N_{out} versus input signal-to-noise ratio, from which L_{conv} can be deduced, is shown in Fig. 7. The apparent tendency toward smaller implementation loss evident at low input S/N is an artifact. These curves were made with constant $S_{in}=-10$ dBm. Low input S/N, therefore, corresponds to large N_{in}. For N_{in} greater than $+6$ dBm ($S_{in}/N_{in}<-16$ dB) the effects of saturation are discernible in Fig. 7 as a variation in the apparent implementation loss. This is a result of the separate application of S_{in} and N_{in} while measuring C_{out} and N_{out}, as described above.

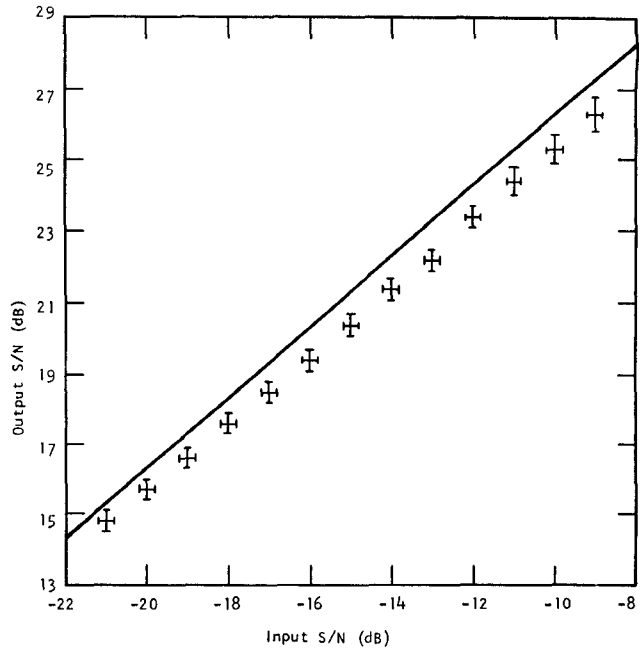

Fig. 7. Convolver output signal-to-noise ratio versus input signal-to-noise ratio for a typical convolver board channel. The error bars represent the repeatability of the measurements. There is an additional estimated uncertainty of ± 0.5 dB in the measurements. The effects of saturation are evident at low input signal-to-noise levels.

The $\simeq$50-dB dynamic range shown in Table I is more than adequate to support the $\simeq$30-dB processing gain of the subsystem. The major sources of the $\simeq$1-dB contribution to the implementation loss by the convolvers and waveform generators are spatial nonuniformities in the convolvers, variations from ideal flat-amplitude, linear-phase performance at the convolver inputs and outputs, and residual distortions in the MSK waveforms. Spatial nonuniformities are the result of geometric and electric factors [8] and result in an unequal weighting in amplitude and phase of the contributions to the output from different parts of the convolver. Additional losses, probably relatively minor, are contributed by the amplifiers, bandpass filters, hybrids, and switches that make up the rest of the subsystem. The total $\simeq$1-dB contribution to implementation loss by the convolvers and waveform generators is quite low considering the BT product of the subsystem. The relatively low distortion levels introduced by the subsystem can be further illustrated by comparing the system output to the calculated theoretical output. The ideal output, illustrated in Fig. 8(a) using the same scale as used in Fig. 3 for the measured output, would be proportional to the autocorrelation function of the SAW MSK filter impulse response $h(t)$ (see (A1) in the Appendix). There are significant discrepancies between Figs. 3 and 8(a). Most notably, the measured output is about 30 ns between nulls, compared to 22 ns for Fig. 8(a). In Fig. 8(b) the autocorrelation function of the ideal MSK filter response, distorted by two SAW transducers centered at f_0, one 3 wavelengths

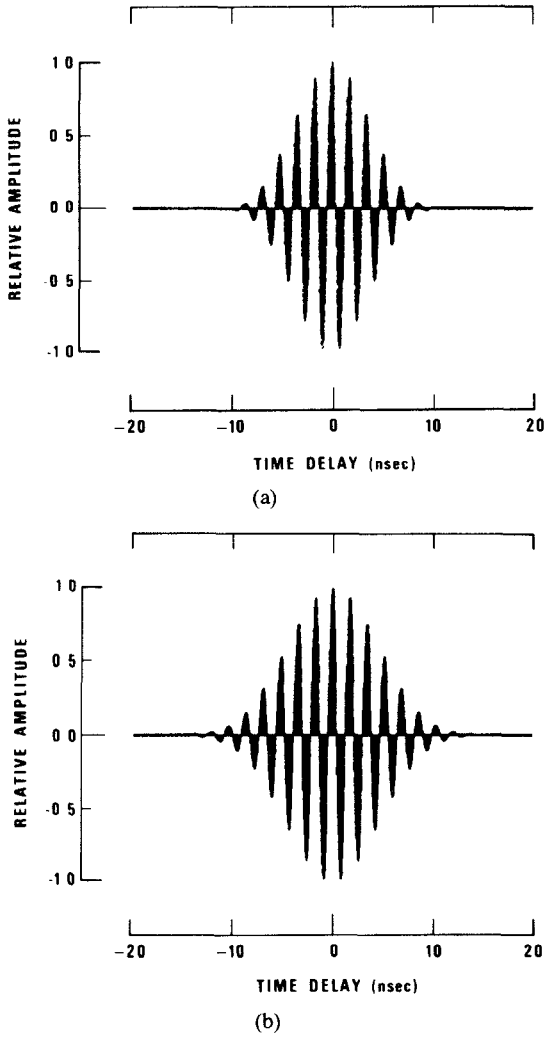

Fig. 8. (a) Calculated matched filter output with ideal MSK inputs. (b) Calculated matched filter output including distortions due to MSK filter output and convolver input transducers.

long and one 2.5 wavelengths long, is displayed on the same scale as used in Figs. 3 and 8(a). These distortions model the effects of the broad-band transducers in the MSK filter outputs and the convolver inputs. The matching networks at the convolver inputs are not accounted for by this calculation. The agreement between Figs. 3 and 8(b) is excellent. The major discrepancy—a slight variation in the apparent period from one cycle to the next in Fig. 8(b)—might be due to time jitter in the test equipment or subsystem distortions not accounted for in Fig. 8(b). Thus virtually all of the deviation from the ideal output pulse shape can be accounted for by a well-understood mechanism—the effect of broad-band SAW transducers. No significant system-level performance degradation appears to result from these small distortions.

V. Conclusions

A SAW convolver-based spread spectrum communications subsystem has been fabricated with >30-dB processing gain, a 92.5-MHz chipping rate, and a 91-kHz data rate. Low-distortion MSK waveforms have been generated with the aid of a SAW filter that compensates for distortions in the waveform generator electronics. Highly developed acoustoelectric convolvers have made possible the achievement of low-distortion levels, near-ideal DPSK data demodulation, 50-dB dynamic range, and contributions to implementation loss of approximately 1 dB. The subsystem thus provides a powerful basis for a spread spectrum communications system.

Appendix
Generation of MSK Waveforms Using a Compensated SAW Filter

The conceptual basis for the MSK modulator is given by the block diagram outlined in Fig. 2(a). The impulse generator creates positive and negative pulses, at a rate $f_c = 1/T_c$, following the chip code. The nth element of the chip code is denoted by C_n, where C_n is 1 or 0 and the nth impulse has amplitude $(-1)^{C_n}$ and is denoted by $\delta_n(t)$. The impulse generator output is applied to a SAW filter with a nominal impulse response chosen so that the filter output will be an MSK waveform. With an ideal impulse generator this impulse response is given by

$$h(t)=\begin{cases}\sin\left[\pi t/(2T_c)\right]\sin(2\pi f_0 t), & 0\leqslant t\leqslant 2T_c\\ 0, & |t-T_c|>T_c.\end{cases} \tag{A1}$$

As shown in Fig. 9, $h(t)$ is a sinusoidal carrier inside one-half cycle of a sinusoidal envelope. The carrier frequency f_0 is chosen so that an odd number of half cycles occur in the time $2T_c$

$$f_0=(2k+1)/(4T_c). \tag{A2}$$

In the case illustrated here, $k=6$. Trigonometric identities can be applied to show that the SAW MSK filter impulse response, $h(t)$, can also be considered as the sum of two time-gated sinusoids

$$h(t)=\begin{cases}\left[\cos(2\pi f_1 t)-\cos(2\pi f_2 t)\right]/2, & 0\leqslant t\leqslant 2T_c\\ 0, & |t-T_c|>T_c\end{cases} \tag{A3}$$

where

$$f_1=f_0-1/(4T_c) \tag{A4a}$$

$$f_2=f_0+1/(4T_c). \tag{A4b}$$

The output of the MSK filter is

$$\sum_n h_n(t) \tag{A5a}$$

where

$$h_n(t)=\delta_n(t)\otimes h(t) \tag{A5b}$$

is the response of the SAW device to the nth impulse generator output. Ideally, $\delta_n(t)$ is $(-1)^{C_n}$ times a δ function centered at t_n

$$t_n=nT_c \tag{A6a}$$

$$\delta_n(t)=(-1)^{C_n}\delta(t-t_n). \tag{A6b}$$

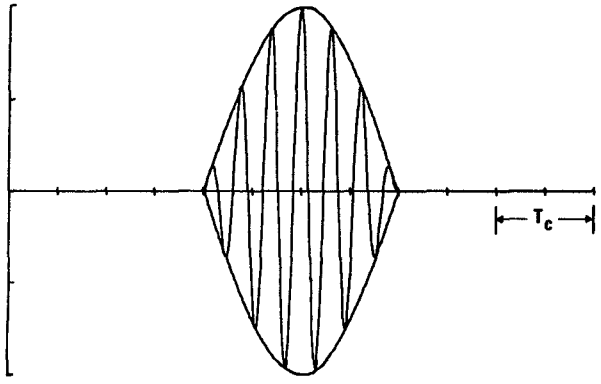

Fig. 9. Impulse response $h(t)$ of the SAW MSK filter required with an ideal impulse generator.

In this case

$$h_n(t)=(-1)^{C_n}h(t-t_n). \tag{A6c}$$

Since the duration of $h(t)$ is $2T_c$ and the time between impulses is T_c, the filter output, (A5a) contains nonzero contributions $h_n(t)$ and $h_{n+1}(t)$

$$\begin{aligned}h_n(t)&=(-1)^{C_n}\sin\left[\pi(t-t_n)/(2T_c)\right]\sin\left[2\pi f_0(t-t_n)\right]\\&=(-1)^{C_n}\left\{\cos\left[2\pi f_1(t-t_n)\right]-\cos\left[2\pi f_2(t-t_n)\right]\right\}/2\end{aligned} \tag{A7}$$

and

$$\begin{aligned}h_{n+1}(t)&=(-1)^{C_{n+1}}(-1)^k\cos\left[\pi(t-t_n)\right.\\&\quad\left./(2T_c)\right]\cos\left[2\pi f_0(t-t_n)\right]\\&=(-1)^{C_{n+1}}(-1)^k\left\{\cos\left[2\pi f_1(t-t_n)\right.\right.\\&\quad\left.\left.+\cos\left[2\pi f_2(t-t_n)\right]\right\}/2\end{aligned} \tag{A8}$$

during the interval

$$t_{n+1}=t_n+T_c\leqslant t\leqslant t_n+2T_c=t_{n+1}+T_c. \tag{A9}$$

Equation (A7) was simplified using trigonometric identities, (A1) and (A3), and the relation (from A6a))

$$t_{n+1}=t_n+T_c. \tag{A10}$$

The output of the SAW MSK filter during the time interval of (A9) is, therefore, given by the sum of (A7) and (A8)

$$\begin{aligned}f_{\mathrm{MSK}}(t)&=h_n(t)+h_{n+1}(t)=(-1)^{C_{n+1}}(-1)^k\\&\quad\cdot\cos\left\{2\pi\left[f_0-(-1)^{C_n+C_{n+1}+k}/(4T_c)\right]\right\}.\end{aligned} \tag{A11}$$

For the case illustrated here, $k=6$ and, therefore, during the interval of (A9)

$$f_{\mathrm{MSK}}(t)=\begin{cases}(-1)^{C_{n+1}}\cos\left[2\pi f_1(t-t_n)\right], & C_n=C_{n+1}\\(-1)^{C_{n+1}}\cos(2\pi f_2(t-t_n)], & C_n\neq C_{n+1}.\end{cases} \tag{A12}$$

The MSK waveform is a uniform amplitude sinusoid with a "local" frequency that takes one of two values, f_1 or f_2, depending on the relation between successive elements of the chip code. Transitions between f_1 and f_2 occur at times $t_n=nT_c$ when the waveform, a cosine function, is at its peak. At this point, for any frequency, the derivative of the cosine function is zero and thus the MSK waveform is continuous and has a continuous first derivative.

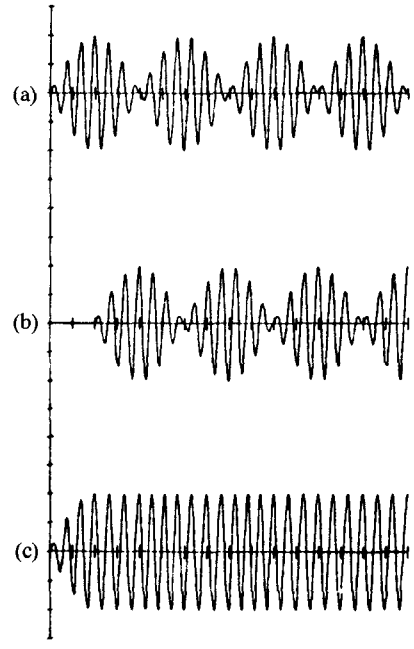

Fig. 10. Formation of the MSK waveform. (a) In-phase chips with code +1,0,1,1. (b) Quadrature chips with code +1,0,1,1. (c) MSK waveform for code 11001111.

The ideal operation of the system is summarized in Fig. 10 for the particular chip code 11001111. The odd-numbered chips, $C_1, C_3, \cdots$, generate the SAW MSK filter output shown on the top line of Fig. 10 and the even-numbered chips generate the output shown on the second line. Note that both the carrier and the envelope of the even-chip waveform are in quadrature with the corresponding features of the odd-chip waveform. The device output, shown on the third line of Fig. 10, is the sum of the first two lines. Note that at all times (following the one-chip long start-up period) one odd-numbered (or in-phase) chip and one even-numbered (or quadrature chip contribute to the output.

The output of an optimized impulse generator is illustrated in Fig. 11(a). The pulses exhibit good uniformity of amplitude and timing. However, the minimum pulsewidth achieved, using Fairchild 100K series ECL components, was 1.6 ns at the pulse base. The corresponding frequency spectrum, illustrated in Fig. 11(b), has a non-negligible rolloff in this band. Therefore, when an uncompensated SAW MSK filter is used with this impulse generator, significant distortion of the MSK waveform results, as shown in Fig. 5(a). The two-step character of the waveform in Fig. 5(a) is consistent with the hypothesis that the impulse generator rolloff is the dominant source of distortion. Regions with "local" frequency $f_1=277.5$ MHz ex-

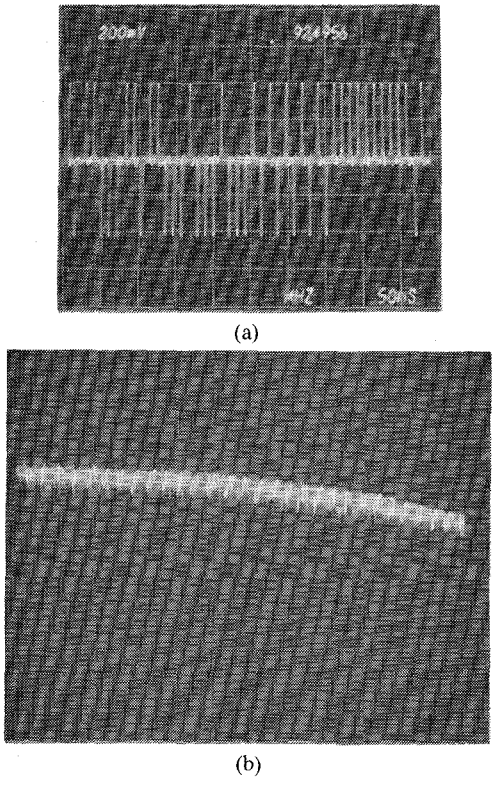

(a)

(b)

Fig. 11. Output of the MSK modulator impulse generator. (a) Time domain, 50 ns per horizontal division. (b) Frequency domain, 300 MHz at center of picture, 20 MHz per horizontal division, 10 dB per vertical division.

hibit higher amplitude than regions with "local" frequency $f_2 = 323.7$ MHz. Computer modeling based on this argument gave good agreement with observed MSK waveforms, indicating that the impulse generator rolloff was the dominant distortion mechanism.

In order to reduce the MSK distortions, the rolloff of the impulse generator spectrum was compensated by a rollup in the SAW MSK filter spectrum [6]. The pulse outputs $\delta_n(t)$ of the impulse generator all have nearly the same shape, denoted by $p(t)$

$$\delta_n(t) = (-1)^{C_n} \times p(t - t_n). \tag{A13}$$

The Fourier transform of $p(t)$ is denoted $P(\omega)$. The ideal MSK spectrum is proportional to $H(\omega)$, the Fourier transform of $h(t)$. By the convolution theorem and (A5b) and A13), the spectrum of the waveform resulting from application of the impulse generator output to an ideal SAW MSK filter is proportional to

$$H_1(\omega) = P(\omega) \times H(\omega). \tag{A14}$$

Ideal MSK would, therefore, be generated if the ideal MSK filter were replaced by a filter with a transfer function $H_c(\omega)$ given by

$$H_c(\omega) = H(\omega)/P(\omega). \tag{A15}$$

A compensated filter was designed to follow (A15) in amplitude exactly at f_1 and f_2 and approximately throughout the remainder of the MSK band. No phase compensation was attempted. The compensated SAW MSK filter utilized in-phase and quadrature weighting in a 6.5 wavelength long apodized transducer on yz-$LiNbO_3$. The second transducer in the compensated MSK filter was a 3 wavelength long broad-band transducer that introduced only minor distortions (<3 percent AM) in the MSK waveform. As much as 4.6-dB rolloff between f_1 and f_2 was successfully compensated in the course of the development work. In the final modules, with an optimized impulse generator, only 1.8 dB of rolloff compensation was required. Fig. 5(b) shows the MSK output of a system that utilized a compensated SAW MSK filter. Amplitude modulation in this case was reduced to $\simeq 7$ percent, with $\simeq$ 13 percent typical in the 8 channels made.

ACKNOWLEDGMENT

The authors wish to give thanks to J. L. Norris, R. C. Bennett, M. A. Heard, and D. T. Bell for their contributions to this work; to S. A. Reible, J. H. Cafarella, I. Yao, and E. Stern for their contributions to the development of convolvers and convolver based systems; to R. S. Wagers for his guidance; to J. R. Jennings and C. F. Shaffer for their work in fabricating the devices and subsystems; and to D. L. Carroll and G. K. Ellis for drafting the figures.

REFERENCES

[1] W. C. Wang, "Signal generation via nonlinear interaction of oppositely directed sonic waves in piezoelectric semiconductors," *Appl. Phys. Lett.*, vol. 18, pp. 337–338, Apr. 1971.

[2] G. S. Kino, W. R. Shreve, and H. R. Gautier, "Parametric interactions of Rayleigh waves," in *1972 Ultrasonics Symp. Proc.* IEEE Cat. No. 71 CHO708-8SU, pp. 285–287.

[3] J. H. Cafarella, W. M. Brown, E. Stern, and J. A. Alusow, "Acoustoelectric convolvers for programmable matched filtering in spread-spectrum systems," *Proc. IEEE*, vol. 64, no. 5, pp. 756–759, May 1976.

[4] D. Brodtkorb and J. E. Laynor, "Fast synchronization in a spread spectrum system based on acoustoelectric convolvers," in *1978 Ultrasonics Symp. Proc.* IEEE Cat. No. 78CH1344-1SU, pp. 561–566.

[5] S. A. Reible, J. H. Cafarella, R. W. Ralston, and E. Stern, "Convolvers for DPSK demodulation of spread spectrum signals," in *1976 Ultrasonics Symp. Proc.* IEEE Cat. No. 76CH1120-5SU, pp. 451–455.

[6] D. C. Malocha, J. H. Goll, and M. A. Heard, "Design of a compensated SAW filter used in a wide spread MSK waveform generator," in *1979 Ultrasonics Symp. Proc.* IEEE Cat. No. 79CH1482-9SU.

[7] J. H. Goll and N. J. Tolar, "Improved efficiency of high BT product SAW convolvers," in *1977 Ultrasonics Symp. Proc.* IEEE Cat. No. 77CH1264-1SU pp. 469–471.

[8] J. H. Goll and R. C. Bennett, "Reactive output tuning of high BT product SAW convolvers," in *1978 Ultrasonics Symp. Proc.* IEEE Cat. No. 78CH1344-1SU, pp. 44–47.

[9] S. A. Reible, K. L. Wang, and V. S. Dolat, "Transverse modes in accoustoelectric convolvers," *1978 Ultrasonics Symp. Proc.* IEEE Cat. No. 78CH1344-ISU, pp. 48–52.

[10] I. Yao and S. A. Reible, "Wide bandwidth acoustoelectric convolvers," in *1979 Ultrasonics Symp. Proc.* IEEE Cat. No. 79CH1482-9SU.

[11] S. A. Reible, "Acoustoelectric Convolver technology for spread-spectrum communications," this issue, pp. 463–473.

[12] R. E. Kahn, S. A. Gronemeyer, J. Bunchfiel, and R. C. Kunzelman, "Advances in packet radio technology," *Proc IEEE*, vol. 66, no. 11, pp. 1468–1496, Nov. 1978.

[13] H. Taub and D. L. Schilling, *Principles of Communications System*. New York: McGraw-Hill, 1971, pp. 224–227, 378–380.
[14] R. C. Dixon, *Spread Spectrum Systems*. New York: Wiley, 1976, p. 235.
[15] M. L. Doelz and E. T. Heald, "Minimum-shift data communication system," US Patent 2 977 417, Mar. 28, 1961.
[16] C. E. Cook and M. Bernfeld, *Radar Signals: An Introduction to Theory and Applications*. New York: Academic Press, 1967, pp. 18–23.
[17] A. K. Jain and R. K. Marston, "Surface acoustic wave apparatus," US Patent 3 969 590, July 13, 1976.
[18] W. R. Smith, "SAW filter for CPSM spread spectrum communications," in *1977 Ultrasonics Symp. Proc.* IEEE Cat. No. 77CH1264-1SU, pp. 524–528.

Wide-Band Signal Processing Using the Two-Beam Surface Acoustic Wave Acoustooptic Time Integrating Correlator

MICHAEL W. CASSEDAY, NORMAN J. BERG, MEMBER, IEEE, IRWIN J. ABRAMOVITZ, AND JOHN N. LEE, MEMBER, IEEE

Abstract—**A new acoustooptic architecture for performing real-time correlation of high-frequency wide-band signals has been developed. It uses a surface-acoustic-wave (SAW) delay line, and features the optical interference of two coherent light beams which have been Bragg-diffracted by SAW's propagating in the line. The signal multiplication, and subsequent time integration of the product formed, is performed by a photodiode array which detects the diffracted light. This architecture has achieved time–bandwidths products exceeding 10^6 (34 MHz×30 ms), and has several attributes which make it particularly well suited for use as a spread-spectrum signal processor. These include linearity of operation, large dynamic range, a large time aperture over which the correlation can be observed, and the ability to determine the center frequency and bandwidth of the signals. A correlator with this architecture has been used to detect a number of wide-band spread-spectrum signals. Its suitability for use as a signal processor in several spread-spectrum systems is considered.**

I. INTRODUCTION

SEVERAL present-day radio systems used for communications, navigation, and radar make use of spread-spectrum techniques to obtain greater range, multiple user access, better range resolution, lower probability of intercept, and improved antijam capability [1, ch.1]. The transmitted signal in these systems is spread over a frequency band that is much larger than is necessary for the information being sent. In most systems of interest, this bandwidth spreading is accomplished by using a special signal in addition to the information being sent to modulate the radio carrier. At the receiver, a correlation demodulation process "collapses" the excess bandwidth, obtaining the improved performance in the system. The wide-band signals employed in these systems present special problems in real-time signal detection and reception, problems which a large time–bandwidth product correlator may help solve.

Current digital processors are too limited in bandwidth to successfully perform real-time correlation of many of these spread-spectrum signals. The "traditional" analog correlator (which consists of a mixer-multiplier followed by an operational amplifier integrator) can process long duration wide-band signals. However, its output represents the correlation of the signals at only one relative time delay between them. It is very desirable to have a correlator which can simultaneously perform the correlation of the signals over a range of relative time delays, thereby sim-

Manuscript received February 15, 1980.
M. W. Casseday, N. J. Berg, and I. J. Abramovitz are with Harry Diamond Laboratories, Adelphi, MD 20783.
J. N. Lee was with the Harry Diamond Laboratories, Adelphi, MD. 02783. He is now with the Naval Research Laboratory, Washington, DC.